

CHALMERS
UNIVERSITY OF TECHNOLOGY

Fast Scattering Analysis of Large Open-Cavity Based Reflectarrays Using a Hybrid Method of Moment and Physical Optics Approach

Downloaded from: https://research.chalmers.se, 2026-11-22 17:39 UTC

Citation for the original published paper (version of record):
Lin, D., Manholm, L., Talcoth, O. et al (2025). Fast Scattering Analysis of Large Open-Cavity Based Reflectarrays Using a Hybrid Method of
Moment and Physical Optics Approach. Proceedings of the International Conference on Electromagnetics in Advanced Applications, ICEAA: 682-686.
http://dx.doi.org/10.1109/ICEAA65662.2025.11305957

N.B. When citing this work, cite the original published paper.

© 2025 IEEE. Personal use of this material is permitted. Permission from IEEE must be obtained for all other uses, in any current or future media, including reprinting/republishing this material for advertising or promotional purposes, or reuse of any copyrighted component of this work in other works.

(article starts on next page)

Fast Scattering Analysis of Large Open-cavity Based Reflectarrays Using a Hybrid Method of Moment and Physical Optics Approach

Dijun Lin*†, Lars Manholm†, Oskar Talcoth†, Sam Agneessens†, Parisa Aghdam†, Rob Maaskant*
* Department of Electrical Engineering, Chalmers University of Technology, Gothenburg, Sweden
{dijun, rob.maaskant}@chalmers.se
† Ericsson Research, Gothenburg, Sweden
{dijun.lin, lars.manholm, oskar.talcot, sam.agneessens, parisa.aghdam}@ericsson.com

***Abstract*—This paper introduces a hybrid modeling approach for the fast analysis of large reflectarrays. The scattering from a 3-D all-metal reflectarray is modeled by a Perfect Electric Conductor (PEC) sheet with impressed aperture magnetic current sources. These currents are obtained by analyzing the aperture fields of isolated unit cells through the method of moments. The induced electric current on the large PEC sheet is then computed through the Physical Optics (PO) approach, thereby reducing the computational complexity from $\mathcal{O}(N^3)$ for classical MoM to $\mathcal{O}(N)$ for PO. The results show, compared to CST, that the total scattered field yields an error of max. 0.32 dB in the main lobe direction for a 5×5 reflectarray with peak gain of 21.8 dB. Furthermore, the relative error related to the PO approach is less than 0.13 dBi, which confirms the validity of the hybrid modeling approach.**

***Index Terms*—method of moment, physical optics, reflectarray, waveguide array**

I. Introduction

ELECTROMAGNETIC surfaces, such as reflectarrays, are typically used for (multi)beam-forming and side-lobe-level control due to their ability to manipulate electromagnetic waves [1]–[3]. Initial designs often rely on the use of periodic boundary conditions implying infinitely large arrays under plane wave incidence. While this approach speeds up simulations, it fails to accurately model mutual coupling, edge effects and a non-planar phase front, leading to inaccuracies in the scattered field pattern.

Reflectarrays are often very large, making them difficult to solve directly due to their increased complexity. In order to reduce the problem size, domain decomposition methods (DDMs) are often proposed that are based on surface equivalence principles [4], [5]. Many Method-of-Moment (MoM) based DDMs have been proposed employing electric field integral equations (EFIEs) and magnetic field integral equations [6]–[9]. Although these methods can solve large problems and have produced accurate results, MoM methodologies typically require Gaussian elimination, which renders it an $\mathcal{O}(N^3)$ complexity problem [10].

This paper proposes to apply Schelkunoff's equivalence for modeling cavity array scattering problems, such as reflectarrays with waveguide cells [11]–[13]. We propose to characterize the unit cell in isolation before modeling the behaviour of the array. Unlike an infinite periodic array methodology, which is limited to uniformly spaced array elements, our approach can model non-uniformly distributed and unique reflectarray elements. Additionally, our method differs from the aforementioned MoM-based methodologies by using Schelkunoff's equivalence combined with zero back current leading to a geometry dimension reduction. The so-obtained PEC sheet

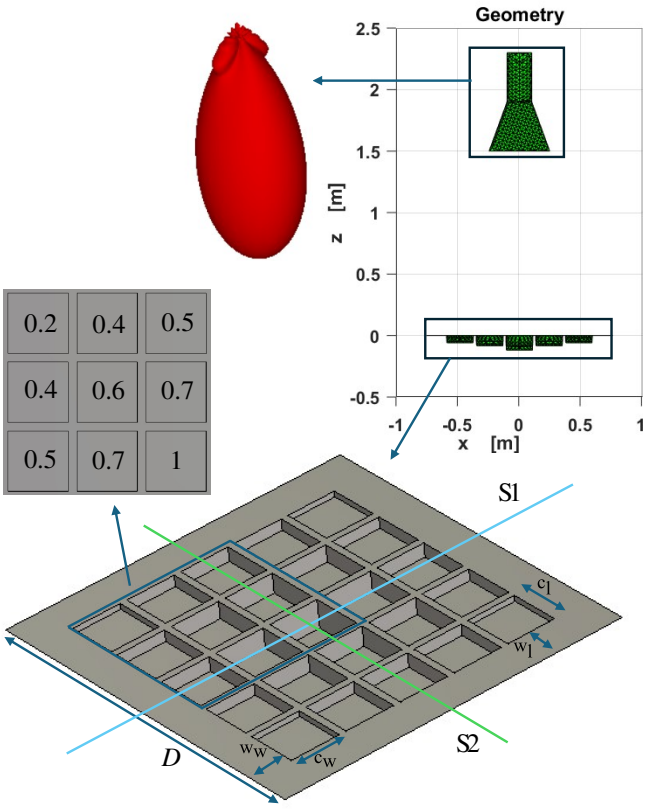


Fig. 1. The CST geometric model (bottom) used to validate the proposed model (top-right). The dimensions are $D = 5C_l + 2W_l + 0.4\lambda$, $C_l = C_w = \lambda/\sqrt{2}$, $W_l = W_w = 0.55\lambda$ and the height for the centre element is 0.397λ. All other elements are modulated in height with quadrant symmetry by symmetry lines S1 and S2, and the subarray shows the relative height modulation coefficient, where the cell height is relative modulation$\times 0.397\lambda$.

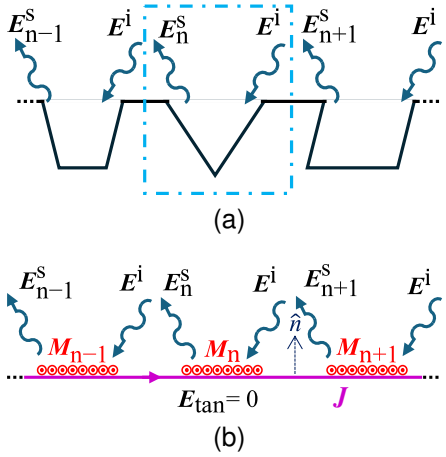


Fig. 2. (a) Original reflectarray configuration. (b) Final configuration with set of aperture magnetic currents and induced electric current on a sheet with imposed PEC boundary condition (all sources radiate in free space).

will prevent internal resonance issues, which are known to occur when only EFIE is used for closed cavities [14, p. 29]. Additionally, using the *physical equivalent* [15, p. 337], the PEC body is removed and replaced by an electric source current representing the induced PEC current. This current can be approximated by the Physical Optics (PO) current to solve for the fields on the front side due to the feed illumination and aperture radiation [16]. PO eliminates the need to calculate matrix inverses, reducing the problem complexity from $\mathcal{O}(N^3)$ to $\mathcal{O}(N)$.

The remainder of this article is organized as follows: In Sec. II, the general methodology is explained, including the setup of the EFIE for single cell analysis, geometry dimension reduction, and Physical Optics boundary conditions. In Sec. III, the validation results are discussed from our in-house MoM solver against those obtained from CST's integral equation (IE) solver. Finally, Sec. IV concludes and provides recommendations for future work.

II. Methodology

Fig. 2a shows a simplified visualization of a cavity based reflectarray with $\boldsymbol{E}^{\text{i}}$ the electric field from an external source (feed) incident on the reflectarray and $\boldsymbol{E}^{\text{s}}_n$ is the scattered field from only the nth array element (see blue dashed box). This isolated element approach significantly reduces the problem size for the EFIE. This fast analysis is repeated for all unit cells, which is explained in detail later. The final goal of the methodology is to represent the original array in Fig. 2a using Schelkunoff's equivalence principle followed up by a geometry dimension reduction step and the application of the *physical equivalent* theorem to arrive at the array model as shown in Fig. 2b.

The scattered field $\boldsymbol{E}^{\text{s}}(\boldsymbol{J},\boldsymbol{M})$ in the final configuration in Fig. 2b is due to the total impressed magnetic current $\boldsymbol{M}$, which is the array of magnetic currents representing the aperture fields, and the electric (source) current $\boldsymbol{J}$ representing the induced current on the PEC in the presence of $\boldsymbol{M}$ and the

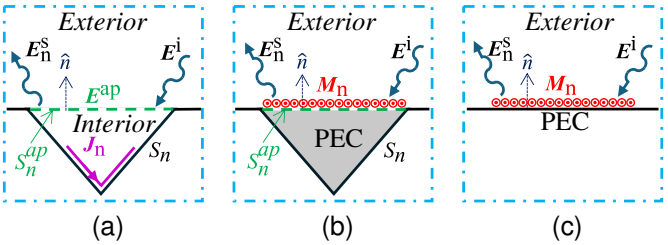


Fig. 3. (a) Original unit cell extracted from 2a with $\boldsymbol{E}^{\text{ap}}$ sampled at aperture S_n. (b) Equivalence principle converting $\boldsymbol{E}^{\text{ap}}$ at the aperture to a magnetic current source $\boldsymbol{M}_n$ for a single cell by closing the cavity with PEC. (c) After removal of the back geometry, effectively flattening the structure, $\boldsymbol{M}_n$ represents the same cell scattering behavior on an infinitely thin PEC sheet

feed. The scattered field is given by [17][1]

$$\boldsymbol{E}^{\text{s}}(\boldsymbol{J},\boldsymbol{M}) = \mathcal{L}(\boldsymbol{J}) - \mathcal{K}(\boldsymbol{M}) + \frac{\hat{\boldsymbol{n}}\times\boldsymbol{M}}{2} \tag{1a}$$

$$\boldsymbol{H}^{\text{s}}(\boldsymbol{J},\boldsymbol{M}) = \frac{1}{\eta_0^2}\mathcal{L}(\boldsymbol{M}) + \mathcal{K}(\boldsymbol{J}) - \frac{\hat{\boldsymbol{n}}\times\boldsymbol{J}}{2} \tag{1b}$$

where the operators

$$\mathcal{L}(\boldsymbol{X}) = -\,j\omega\mu_0 \text{ p.v.} \iint_s \boldsymbol{X}(\boldsymbol{r}')G(\boldsymbol{r}-\boldsymbol{r}')dS' + \frac{1}{j\omega\epsilon_0}\boldsymbol{\nabla} \text{ p.v.} \iint_s \boldsymbol{\nabla}'\cdot\boldsymbol{X}(\boldsymbol{r}')G(\boldsymbol{r}-\boldsymbol{r}')dS' \tag{2a}$$

$$\mathcal{K}(\boldsymbol{X}) = \text{p.v.} \iint_s \boldsymbol{X}(\mathbf{r}')\times\boldsymbol{\nabla}'G(\boldsymbol{r}-\boldsymbol{r}')dS' \tag{2b}$$

and where $G = e^{-jk_0R}/(4\pi R)$. Furthermore, $R = |\boldsymbol{r}-\boldsymbol{r}'|$ and the wavenumber $k_0 = \omega\sqrt{\mu_0\epsilon_0}$. The operators integrate over the support of the surface current.

A. Isolated Cell Analysis

In an isolated cell (blue dashed box), see Fig. 3a, only the geometry of a single cell is considered. To compute the induced electric current $\boldsymbol{J}_n$ on the interior region of the nth cell, the PEC boundary condition $\boldsymbol{E}_{\text{tan},n} = \boldsymbol{E}^{\text{i}}_{\text{tan}} + \boldsymbol{E}^{\text{s}}_{\text{tan},n}(\boldsymbol{J}_n) = \boldsymbol{0}$ is imposed, i.e.,

$$-\boldsymbol{E}^{\text{s}}_{\text{tan},n}(\boldsymbol{J}_n) = \boldsymbol{E}^{\text{i}}_{\text{tan}} \quad \boldsymbol{r}\in S_n \tag{3}$$

Next, $\boldsymbol{J}_n$ is expanded into $P^{[n]}$ RWG basis functions $\{\boldsymbol{f}^{[n]}_p\}_{p=1}^{P^{[n]}}$ [18], i.e.,

$$\boldsymbol{J}_n(\boldsymbol{r}) = \sum_{p=1}^{P^{[n]}} I^{[n]}_p \boldsymbol{f}^{[n]}_p(\boldsymbol{r}) \tag{4}$$

where $\{I^{[n]}_p\}$ is the associated set of expansion coefficients. Following Galerkin's moment method, the EFIE in (3) is tested $P^{[n]}$ times through the symmetric product $\langle \boldsymbol{a},\boldsymbol{b}\rangle = \iint \boldsymbol{a}\cdot\boldsymbol{b}\,dS$ and (3) results in the matrix equation

$$\mathbf{Z}^{[n]}\mathbf{I}^{[n]} = \mathbf{V}^{[n]} \tag{5}$$

where

$$Z^{[n]}_{pq} = -\langle \boldsymbol{f}^{[n]}_p, \mathcal{L}(\boldsymbol{f}^{[n]}_q)\rangle \tag{6a}$$

$$V^{[n]}_p = \langle \boldsymbol{E}^{\text{i}}, \boldsymbol{f}^{[n]}_p\rangle \tag{6b}$$

[1]Eq. (2) in [17] contains a minus sign error in front of the normal vector.

for $q = 1, 2, \ldots, P^{[n]}$. After obtaining the coefficient vector $\mathbf{I}^{[n]}$ by solving (5), one can compute the electric field on the aperture $\boldsymbol{E}^{\text{ap},[n]} = \boldsymbol{E}^{\text{s}}(\boldsymbol{J}_n) + \boldsymbol{E}^{\text{i}}$, where $\boldsymbol{J}_n$ is known and expanded in terms of RWGs as in (4). Using Schelkunoff's equivalence, as seen in Fig. 3b, the magnetic current on the nth aperture is then determined by

$$\boldsymbol{M}_n = \begin{cases} \boldsymbol{E}^{\text{ap},[n]} \times \hat{\boldsymbol{n}} & \boldsymbol{r} \in S_n^{\text{ap}} \\ \mathbf{0} & \text{otherwise} \end{cases} \tag{7}$$

This nullifies the field in the interior region since it is filled with PEC material. Moreover, under the assumption of zero current on the backside of the geometry, one can reduce the geometry to a thin PEC sheet. This allows each cell to be represented as a PEC sheet with impressed $\boldsymbol{M}_n$ as seen in Fig 3c.

B. Array Synthesis

After obtaining the equivalent model representation of the unit cells, Fig. 3c, the cells can be aggregated as seen in Fig 2b. To calculate $\boldsymbol{J}$ on the PEC sheet, or array, the EFIE can be formulated using the PEC boundary condition $\boldsymbol{E}_{\text{tan}} = \boldsymbol{E}^{\text{i}}_{\text{tan}} + \boldsymbol{E}^{\text{s}}_{\text{tan}}(\boldsymbol{M}) + \boldsymbol{E}^{\text{s}}_{\text{tan}}(\boldsymbol{J}) = \mathbf{0}$. Substituting (1) in this boundary condition results in

$$\underbrace{-\mathcal{L}(\boldsymbol{J})|_{\text{tan}}}_{\boldsymbol{E}^{\text{s}}_{\text{tan}}(\boldsymbol{J})} = \boldsymbol{E}^{\text{i}}_{\text{tan}} \underbrace{-\mathcal{K}(\boldsymbol{M})|_{\text{tan}} + \frac{\hat{\boldsymbol{n}} \times \boldsymbol{M}}{2}}_{\boldsymbol{E}^{\text{s}}_{\text{tan}}(\boldsymbol{M})} \tag{8}$$

After expanding the entire array/sheet current $\boldsymbol{J}$ in P RWG basis functions, and testing the EFIE using Galerkin's approach, one obtains

$$\mathbf{ZI} = \mathbf{V} \tag{9}$$

where

$$Z_{pq} = -\langle \boldsymbol{f}_p, \mathcal{L}(\boldsymbol{f}_q) \rangle \tag{10a}$$

$$V_p = \langle \boldsymbol{E}^{\text{i}} + \boldsymbol{E}^{\text{s}}(\boldsymbol{M}), \boldsymbol{f}_p \rangle \tag{10b}$$

for $q = 1, 2, ..., P$, and $\boldsymbol{M}$ is known following Eq. (7).

Alternatively, $\boldsymbol{J}$ can be found faster and more directly using the Physical Optics method, i.e.,

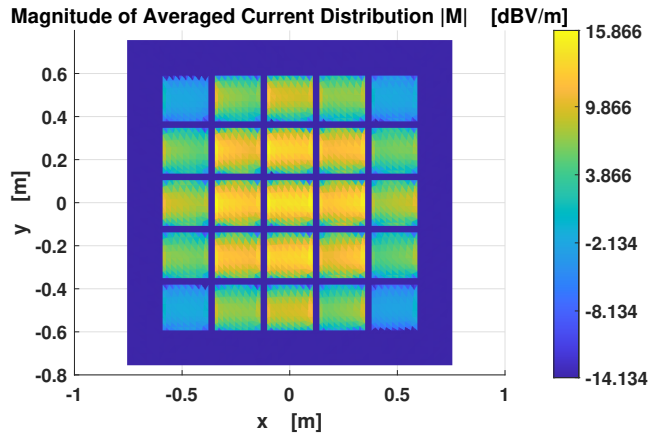
$$\boldsymbol{J} = 2\hat{\boldsymbol{n}} \times (\boldsymbol{H}^{\text{i}} + \boldsymbol{H}^{\text{s}}(\boldsymbol{M})) \tag{11}$$

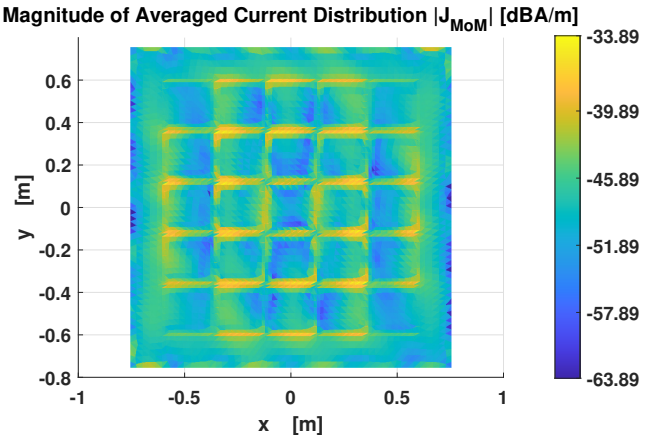
where the error incurred by the PO approximation, which is largest at the array edge, is limited by an upper bound error in directivity [19]:

$$\Delta G \approx 0.22 \left(\frac{\lambda}{D}\right)^2 \quad [\text{dB}] \tag{12}$$

where D represents the smallest diameter of the array. This error diminishes if the reflectarray is significantly larger than the free space wavelength λ. After determining $\boldsymbol{J}$, the overall radiation behaviour of the reflectarray system can be expressed through the total field

$$\boldsymbol{E} = \boldsymbol{E}^{\text{i}} + \boldsymbol{E}^{\text{s}}(\boldsymbol{M}) + \boldsymbol{E}^{\text{s}}(\boldsymbol{J}) \tag{13}$$





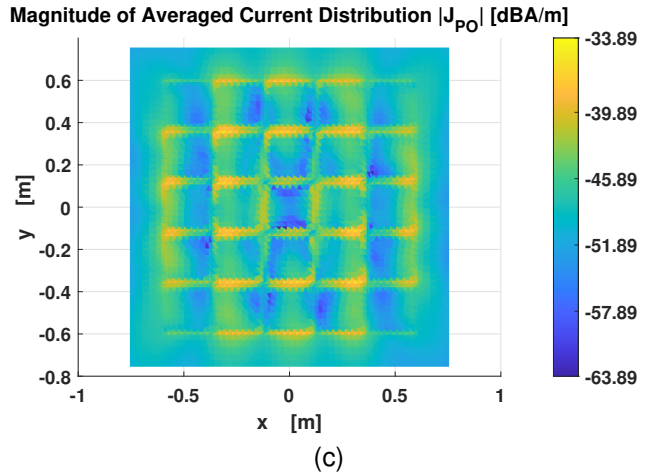
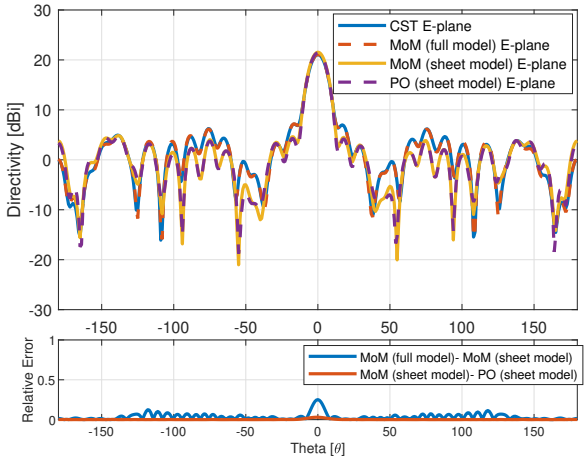


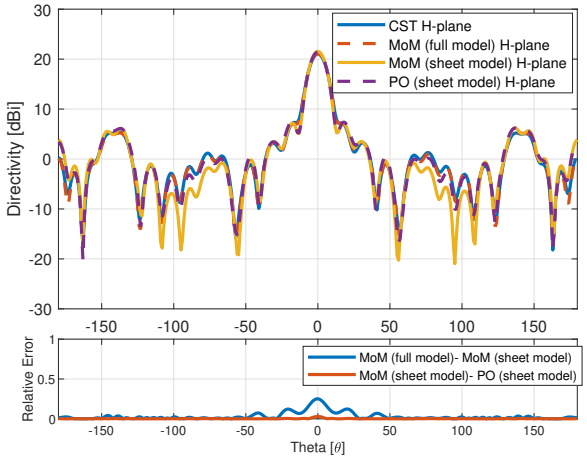
Fig. 4. (a) The aperture magnetic current obtained by sampling single cells. (b) The induced current on the PEC ground plane due to incident fields from the feed and the apertures calculated through MoM. (c) The induced current on the PEC ground plane due to incident fields from the feed and the apertures calculated through PO.

III. Results

The proposed methodology is evaluated on a full metal 5×5 waveguide-based reflectarray with a horn feed as shown in Fig. 1. To demonstrate the methodology's capability to handle various cells, waveguide cells with varying heights are



(a)



(b)

Fig. 5. (a) E-plane and (b) H-plane radiation pattern of the array with their respective relative error per angle of θ in linear scale.

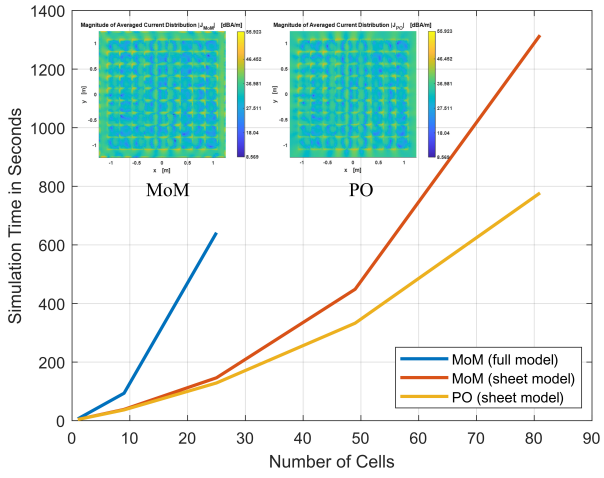


Fig. 6. Time benchmark comparing the simulation time using the full model MoM, the sheet MoM and sheet PO.

used. For simplicity, the coupling between the horn and the array, as well as blockage effects, were neglected. Reference validation was performed using a full MoM solver (=EFIE for the full geometric model), treating the horn as a far-field source. Additionally, CST results were included to confirm the validity of the full MoM solver.

The results are provided for MoM (sheet model), PO (sheet model) and two references; CST (full model), MoM (full model). Fig. 4a illustrates the magnetic currents on the apertures, where one can see the non-uniform illumination of the aperture due to the feed. Fig. 4b displays the induced current on the PEC sheet, calculated using the MoM (sheet model). The PO calculated current is shown in Fig. 4c. The currents in Fig. 4b and 4c match well, except around the edges where PO modeling is less accurate, as expected. This similarity is also observed in the radiation patterns in the E- and H-planes in Fig. 5a and 5b. The scattered field from a 5×5 reflectarray as computed by full MoM approach differs only by 0.043 dB in peak gain (21.1 dBi) w.r.t. CST's integral equation solver. The MoM sheet model increases the error to max. 0.32 dB. Finally, the physical-optics approximation is observed to not increase this error (< 0.129 dB), which shows that the PO approximation yields accurate results once magnetic aperture currents can be accurately determined including coupling effects. Finally, Fig. 6 compares the computation times for the full-wave MoM, reduced model, and PO, indicating that the PO method scales more favorable with increasing number of cells.

IV. Conclusion

The results have demonstrated that the proposed hybrid PO-MoM approach scales more favorable with the increasing complexity of the problem while maintaining good accuracy. Additionally, the geometry reduction to a sheet has little effect on the radiation pattern, as evidenced by the well-matched pattern in the backside direction of the array. This suggests that the discrepancy is directly related to the aperture currents obtained through isolated cell analyses. Overall, the results confirm the validity of using a geometry reduction strategy combined with PO and the MoM for fast calculation of cavity-based reflectarrays.

The present method does not account for full mutual coupling effects between apertures, due to determination of magnetic aperture currents in isolated environment. This issue will be addressed in the future using a generalized admittance matrix approach combined with domain decomposition.

Acknowledgment

This work was funded by the European Union, under ANTERRA 101072363 HORIZON-MSCA-2021-DN-01. Views and opinions expressed are however those of the author(s) only and do not necessarily reflect those of the European Union. Neither the European Union nor the granting authority can be held responsible for them.

REFERENCES

[1] J. Zhu, Y. Yang, S. Liao, and Q. Xue, "Additively Manufactured Metal-Only Waveguide-Based Millimeter-Wave Broadband Achromatic Reflectarrays," *IEEE Transactions on Antennas and Propagation*, vol. 71, no. 7, pp. 6185–6190, Jul. 2023, ISSN: 15582221. DOI: 10.1109/TAP.2023.3278799.

[2] Z. An, T. Makdissy, M. G. Vigueras, S. Vaudreuil, and R. Gillard, "Bandwidth Enhancement of a Metal-Only Reflectarray Based on the Phoenix Cell," in *2022 IEEE International Symposium on Antennas and Propagation and USNC-URSI Radio Science Meeting, AP-S/URSI 2022 - Proceedings*, Institute of Electrical and Electronics Engineers Inc., 2022, pp. 587–588, ISBN: 9781665496582. DOI: 10.1109/AP-S/USNC-URSI47032.2022.9887061.

[3] Z. An, T. Makdissy, M. Garcia-Vigueras, S. Vaudreuil, and R. Gillard, "A Reflector Antenna with Integrated Frequency-Selective Metal-Only Reflectarray for Dual-Band Operation," *IEEE Access*, vol. 11, pp. 127 098–127 106, 2023, ISSN: 21693536. DOI: 10.1109/ACCESS.2023.3331744.

[4] A. Booysen, "Aperture theory and the equivalence theorem," in *IEEE Antennas and Propagation Society International Symposium. 1999 Digest. Held in conjunction with: USNC/URSI National Radio Science Meeting (Cat. No.99CH37010)*, vol. 2, IEEE, pp. 1258–1261, ISBN: 0-7803-5639-X. DOI: 10.1109/APS.1999.789542. [Online]. Available: http://ieeexplore.ieee.org/document/789542/.

[5] R. Harrington and J. Mautz, "A generalized network formulation for aperture problems," *IEEE Transactions on Antennas and Propagation*, vol. 24, no. 6, pp. 870–873, Nov. 1976, ISSN: 0096-1973. DOI: 10.1109/TAP.1976.1141420.

[6] U. R. Patel, P. Triverio, and S. V. Hum, "A Fast Macromodeling Approach to Efficiently Simulate Inhomogeneous Electromagnetic Surfaces," *IEEE Transactions on Antennas and Propagation*, Nov. 2020, ISSN: 15582221. DOI: 10.1109/TAP.2020.3000857.

[7] U. R. Patel, P. Triverio, and S. V. Hum, "A macromodeling approach to efficiently compute scattering from large arrays of complex scatterers," *IEEE Transactions on Antennas and Propagation*, vol. 66, no. 11, pp. 6158–6169, Nov. 2018, ISSN: 0018926X. DOI: 10.1109/TAP.2018.2866509.

[8] R. Gholami, P. Naseri, P. Triverio, and S. V. Hum, "An Efficient Integral Equation Method for Full-Wave Analysis of Inhomogeneous Electromagnetic Surfaces With Connected Conductors," *IEEE Transactions on Antennas and Propagation*, vol. 70, no. 7, pp. 5647–5658, Jul. 2022, ISSN: 0018-926X. DOI: 10.1109/TAP.2022.3145482. [Online]. Available: https://ieeexplore.ieee.org/document/9696224/.

[9] I. Kim, H.-R. Im, I.-P. Hong, H. Lee, and J.-G. Yook, "An Accelerated Method of a Generalized Transition Matrix Model Using Characteristic Basis Functions for Large-Scale Open-Ended Cavities," *IEEE Transactions on Antennas and Propagation*, vol. 72, no. 8, pp. 6813–6818, Aug. 2024, ISSN: 0018-926X. DOI: 10.1109/TAP.2024.3407382. [Online]. Available: https://ieeexplore.ieee.org/document/10550126/.

[10] V. Strassen, "Gaussian elimination is not optimal," *Numerische Mathematik*, vol. 13, no. 4, pp. 354–356, Aug. 1969, ISSN: 0029-599X. DOI: 10.1007/BF02165411.

[11] S. A. Schelkunoff, "Some Equivalence Theorems of Electromagnetics and Their Application to Radiation Problems," *Bell System Technical Journal*, vol. 15, no. 1, pp. 92–112, Jan. 1936, ISSN: 00058580. DOI: 10.1002/j.1538-7305.1936.tb00720.x.

[12] S. A. Schelkunoff, "Kirchhoff's formula, its vector analogue, and other field equivalence theorems," *Communications on Pure and Applied Mathematics*, vol. 4, no. 1, pp. 43–59, Jun. 1951, ISSN: 0010-3640. DOI: 10.1002/cpa.3160040107.

[13] S. Rengarajan and Y. Rahmat-Samii, "The field equivalence principle: illustration of the establishment of the non-intuitive null fields," *IEEE Antennas and Propagation Magazine*, vol. 42, no. 4, pp. 122–128, 2000, ISSN: 10459243. DOI: 10.1109/74.868058.

[14] W. C. Gibson, *The method of moments in electromagnetics*. Chapman & Hall/CRC, 2008, ISBN: 9781420061451.

[15] C. A. Balanis, *Advanced engineering electromagnetics*. John Wiley & Sons, Inc., 2012, ISBN: 978-0-470-58948-9.

[16] J. S. Asvestas, "The physical optics method in electromagnetic scattering," *Journal of Mathematical Physics*, vol. 21, no. 2, pp. 290–299, Feb. 1980, ISSN: 0022-2488. DOI: 10.1063/1.524413.

[17] R. Maaskant, C. Bencivenni, and M. V. Ivashina, "Characteristic basis function analysis of large aperture-fed antenna arrays," in *8th European Conference on Antennas and Propagation, EuCAP 2014*, Institute of Electrical and Electronics Engineers Inc., 2014, pp. 2427–2431, ISBN: 9788890701849. DOI: 10.1109/EuCAP.2014.6902308.

[18] S. Rao, D. Wilton, and A. Glisson, "Electromagnetic scattering by surfaces of arbitrary shape," *IEEE Transactions on Antennas and Propagation*, vol. 30, no. 3, pp. 409–418, May 1982, ISSN: 0018-926X. DOI: 10.1109/TAP.1982.1142818.

[19] P.-S. Kildal, "On the accuracy of physical optics," *IEEE Transactions on Antennas and Propagation*, vol. 30, no. 3, pp. 509–512, May 1982, ISSN: 0096-1973. DOI: 10.1109/TAP.1982.1142809. [Online]. Available: http://ieeexplore.ieee.org/document/1142809/.